

# **Pre-Industrial-Scale Combined Solar Photo-Fenton and Immobilised Biomass Activated-Sludge Bio-treatment**

I. Oller <sup>a</sup>, S. Malato <sup>a,\*</sup>, J.A. Sánchez-Pérez <sup>b</sup>, M.I. Maldonado <sup>a</sup>, W. Gernjak <sup>a</sup>, L.A. Pérez-Estrada <sup>a</sup>, J.A. Muñoz <sup>c</sup>, C. Ramos <sup>c</sup> and C. Pulgarín <sup>d</sup>.

<sup>a</sup> Plataforma Solar de Almería (CIEMAT). Carretera Senés, Km 4. 04200 Tabernas (Almería), Spain.

<sup>b</sup> Departamento de Ingeniería Química, Universidad de Almería, Crta de Sacramento s/n, 04120 Almería, Spain.

<sup>c</sup> DSM-DERETIL. Villaricos (Almería), Spain.

<sup>d</sup> Ecole Polytechnique Fédérale de Lausanne, Institute of Chemical Sciences and Engineering, GGEC, Station 6, CH-1015 Lausanne, Switzerland.

\* Corresponding author: S. Malato: Tel.: +34-950-387940.

Fax: +34-950-365015.

e-mail: [sixto.malato@psa.es](mailto:sixto.malato@psa.es)

## **ABSTRACT**

This paper reports on up-scaling of a new technology combining solar photo-Fenton and aerobic biological processes to successfully treat a saline industrial wastewater containing around  $600 \text{ mg L}^{-1}$  of a non-biodegradable compound ( $\alpha$ -methylphenylglycine, MPG) and Dissolved Organic Carbon (DOC) of between  $400\text{-}600 \text{ mg L}^{-1}$ . Pilot-plant tests were used in designing this demonstration hybrid solar photocatalytic-biological plant with a  $4\text{-m}^3$  daily treatment capacity. It consists of a solar photo-Fenton reactor with  $100 \text{ m}^2$  of solar compound parabolic collectors (CPCs), and an aerobic biological treatment plant based on an immobilised-biomass activated-sludge reactor ( $1 \text{ m}^3$ ). The catalyst concentration was  $\text{Fe}^{2+} = 20 \text{ mg L}^{-1}$ . The overall efficiency in the combined system was around 95% mineralization. 50% of the initial DOC was degraded in the photo-Fenton pre-treatment and 45% was removed in the aerobic biological treatment.

## **Keywords**

Aerobic biological treatment, demonstration plant, saline industrial wastewater, solar photo-Fenton, solar photocatalysis.

## 1. INTRODUCTION

Chemical pollution of surface water can perturb aquatic ecosystems, causing loss of habitats and biodiversity. Humans are exposed to pollution of the aquatic environment by consuming fish or seafood, drinking water and possibly in recreational activities. Pollutants from various sources (e.g. agriculture, industry, incineration) may be released to the environment as products or as unintended by-products, and they may be historical or used daily in household products. In the European Union, water policy is constantly being adapted to protect and improve the quality of Europe's fresh water resources. Article 16 of the Water Framework Directive 2000/60/EC (WFD), for instance, sets out a strategy for dealing with chemical pollution of water.

Although conventional biological treatment is often the most cost-effective alternative, industrial wastewater containing toxic and/or non-biodegradable organic pollutants cannot be treated by biological systems. Therefore, new powerful, clean and safe decontamination technologies must be developed. Among the different treatments available for industrial effluents containing recalcitrant pollutants, Advanced Oxidation Processes (AOPs) have been widely proven to be highly efficient<sup>1-5</sup>. AOPs are characterized by the production of hydroxyl radicals ( $\bullet\text{OH}$ ), which are able to oxidise and mineralise almost any organic molecule, yielding  $\text{CO}_2$  and inorganic ions. Due to the reactivity of hydroxyl radicals, their attack is unselective, which is useful for the treatment of wastewater containing many different contaminants<sup>6</sup>. The use of AOPs for wastewater treatment has been studied extensively, but UV radiation generation by lamps or ozone production is still expensive. Therefore, research is focusing on AOPs which can be driven by solar radiation (photo-Fenton and heterogeneous catalysis with UV/ $\text{TiO}_2$ ), making their development very attractive for practical applications<sup>7-10</sup>. The photo-Fenton process, which combines Fenton (addition of  $\text{H}_2\text{O}_2$  to  $\text{Fe}^{2+}$  salts) and UV-

Vis light<sup>11</sup>, has been demonstrated to be the most promising such technology for treating wastewater containing pollutants at concentrations<sup>12-16</sup> over 10 mg L<sup>-1</sup>, as the reaction rate is usually much faster than TiO<sub>2</sub> photocatalysis and separation of iron is very often unnecessary<sup>17</sup>.

The major drawback of AOPs is that their operating costs exceed those of biological treatment. One of the most attractive approaches for process optimisation in this sense is coupling AOPs with a biological treatment<sup>18-20</sup>. In these integrated systems, AOPs are usually employed as a pre-treatment to enhance the biodegradability of waste water containing recalcitrant or inhibitory pollutants. Recently, very attractive combined systems have been proposed to treat different kinds of industrial wastewater<sup>21-25</sup>.

This work evaluates the technical feasibility of pre-industrial combined solar photo-Fenton/aerobic biological treatment of a highly saline industrial wastewater containing around 600 mg L<sup>-1</sup> of a non-biodegradable compound ( $\alpha$ -methylphenylglycine, MPG) and 400-700 mg L<sup>-1</sup> total organic carbon (DOC). The purpose of this treatment strategy was to achieve sufficient biodegradability of the photo-oxidized effluent to allow its discharge into an aerobic Immobilised Biomass Reactor (IBR). Based on results in pilot plant treatment of the non-biodegradable pollutant (MPG) dissolved in distilled water, model highly saline (NaCl 35 g L<sup>-1</sup>) water<sup>17</sup> and real wastewater<sup>26</sup>, a new hybrid photocatalytic-biological demonstration plant with a 4-m<sup>3</sup> daily treatment capacity was designed and erected on the grounds of a pharmaceutical company located in the south of Spain<sup>27</sup>. Pre-industrial-scale results are compared with those found at pilot plant scale (MPG dissolved in real wastewater) and the overall efficiency of the combined treatment is evaluated.

## 2. MATERIALS AND METHODS

### 2.1. Chemicals.

Technical-grade  $\alpha$ -methylphenylglycine (MPG,  $C_9H_{11}NO_2$ , 100% purity), a bio-recalcitrant by-product produced during synthesis of pharmaceuticals, was used in this study as received (see MPG chemical structure inserted in **Figure 3 (a)**) at a concentration of  $600\text{ mg L}^{-1}$  ( $DOC = 393\text{ mg L}^{-1}$ ) dissolved in the real effluent from an industrial pharmaceutical plant. The composition of this wastewater (without MPG) is typically  $NH_4^+ = 0\text{-}40\text{ mg L}^{-1}$ ,  $NO_3^- = 200\text{-}600\text{ mg L}^{-1}$ ,  $COD = 40\text{-}400\text{ mg L}^{-1}$ ,  $DOC = 20\text{-}200\text{ mg L}^{-1}$ , suspended solids =  $20\text{-}100\text{ mg L}^{-1}$  in seawater  $Cl = 19\text{ g L}^{-1}$ ,  $SO_4^{2-} = 2.7\text{ g L}^{-1}$ ,  $Na = 11\text{ g L}^{-1}$ ,  $Mg = 1.3\text{ g L}^{-1}$ ,  $Ca = 0.5\text{ g L}^{-1}$ ,  $K = 0.4\text{ g L}^{-1}$ , Conductivity =  $55\text{ mS}$ . Photo-Fenton experiments were performed using iron sulphate ( $FeSO_4 \cdot 7H_2O$ ,  $20\text{ mg L}^{-1}$   $Fe^{2+}$ ), reagent-grade hydrogen peroxide (30% w/v) and sulphuric acid for pH adjustment (around 2.3-2.5), all provided by Panreac. The pH of the photo-treated solutions was neutralized prior to bio-treatment and maintained during the biological treatment by automatic adjustment with NaOH (reagent grade, Panreac).

### 2.2 Analytical determinations.

MPG concentration was analysed using reverse-phase liquid chromatography (flow rate  $0.5\text{ ml min}^{-1}$ ) with a UV detector in an HPLC-UV (Agilent Technologies, series 1100) with C-18 column (LUNA  $5\text{ }\mu\text{m}$ ,  $3\text{ mm} \times 150\text{ mm}$  from Phenomenex). The mobile phase composition employed for detecting the pollutant was phosphoric acid at  $50\text{ mM}$  adjusted to pH 2.5 with NaOH, at a wavelength of  $210\text{ nm}$ .

Mineralization was monitored by measuring dissolved organic carbon (DOC) by direct injection of filtered samples into a Shimadzu-5050A TOC analyser provided with an NDIR detector and calibrated with standard solutions of potassium phthalate. Samples

were filtered through 0.22- $\mu\text{m}$ -pore size PTFE syringe-driven filters (Millipore Millex<sup>®</sup> GN).

Ammonium, nitrate and nitrite concentrations in the outlet of the biological treatment were measured by Merck kits (ref: 1.14658.0001 for  $\text{NH}_4^+$ , ref: 1.14542.0001 for  $\text{NO}_3^-$  and ref: 1.14657.001 for  $\text{NO}_2^-$ ).

Hydrogen peroxide in the photo-Fenton experiments was analysed by iodometric titration.

### **2.3. Experimental set-up.**

The demonstration plant designed and erected for the combined solar photo-Fenton / biological treatment of saline non-biodegradable industrial wastewater is made up of a photo-Fenton plant and an aerobic biological system. It was erected on the grounds of a pharmaceutical company located in the south of Spain (see **Figure 1**).

## **FIGURE 1**

### **2.3.1. Solar photo-Fenton plant.**

The solar photo-Fenton reactor consists of a 3000-L buffer or recirculation tank, a centrifugal pump (A4-stainless steel Grunfos, recirculation flow rate of  $11 \text{ m}^3 \text{ h}^{-1}$ ), and  $100\text{-m}^2$  solar collector field made up of three rows of Compound Parabolic Collectors (CPCs) specially developed for photo-Fenton applications. 15 CPC modules were arranged in each row and 50-mm-diameter glass absorber tubes were mounted on an aluminium frame tilted  $37^\circ$  (see **Figure 1 (left)**). The total system volume is 4000 L (1260 L of illuminated volume), with three in-line sensors, pH (Sensolyt probe, WTW), dissolved oxygen (Trioximatic 700IQ probe, WTW) and hydrogen peroxide concentration ( $\text{H}_2\text{O}_2$  Electrode & controller support, ALLDOS,  $0\text{-}2000 \text{ mg L}^{-1}$ ), in the

polypropylene piping (see diagram in **Figure 2**). The pH and oxygen probe insertions in the piping are PVC-C. The buffer tank is a conical-bottomed vessel for settling and removing suspended solids when necessary.

Solar ultraviolet radiation (UV) was measured by a global UV radiometer (KIPP&ZONEN, model CUV 3) mounted on a platform with the same tilt as the collectors. The system is completed by an electric and electronic instrument panel in the field and a PC for on-line data acquisition.

With **Equation 1**, combination of the data from several days' experiments and their comparison with other photocatalytic experiments is possible.

$$t_{30W,n} = t_{30W,n-1} + \Delta t_n \frac{UV}{30} \frac{V_i}{V_T}; \quad \Delta t_n = t_n - t_{n-1} \quad (1)$$

Where  $t_n$  is the experimental time for each sample, UV is the average solar ultraviolet radiation measured during  $\Delta t_n$ , and  $t_{30W}$  is a "normalized illumination time". In this case, time refers to a constant solar UV power of  $30 \text{ W m}^{-2}$  (typical solar UV power on a perfectly sunny day around noon).

Photo-Fenton experiments were carried out by filling the whole plant with saline industrial wastewater (from the pharmaceutical company's wastewater treatment plant), adjusting the pH to 2.3-2.5 (with  $\text{H}_2\text{SO}_4$ ), and adding the pre-dissolved non biodegradable MPG until the desired concentration of  $600 \text{ mg L}^{-1}$  was achieved. Although it is widely known that the optimal pH for photo-Fenton experiments is 2.8-2.9, in this particular case it was reduced to 2.3-2.5 in order to avoid a pH over 2.9 during the treatment, due to MPG nitrogen released as ammonium (see comments in Section 3.1).

This mixture was properly homogenized by turbulent recirculation for half an hour. Then the ferrous iron salt was added ( $20 \text{ mg L}^{-1}$  of  $\text{Fe}^{2+}$ ) and after another 30 minutes of homogenisation, the amount of hydrogen peroxide required according to previous pilot

plant experiments (16 litres which corresponds to 35 mM), was added<sup>26</sup>. Hydrogen peroxide was measured frequently and consumed reagent was replaced (6 litres which corresponds to 13 mM H<sub>2</sub>O<sub>2</sub>) when around 40% of initial DOC was mineralised (see **Figure 3 (a)**). The collectors were always uncovered during homogenisation. Therefore it was not possible to differentiate the quick Fenton reaction at the beginning (when all the iron was as Fe<sup>2+</sup>) from photo-Fenton. In any case, with such a strong concentration of organics (hundreds of mg L<sup>-1</sup> of DOC) and such a low concentration of iron, the effect of the Fenton reaction at the beginning was not very relevant. Indeed, the reaction rate was governed mainly by the slower photochemical reactions, as described in Results and Discussion section with regard to **Figure 3**.

### **2.3.2. Immobilised activated-sludge biotreatment plant.**

The aerobic biological demonstration plant for combined photo-Fenton/Biological experiments consists of three modules, a 5000-L neutralisation tank, a 2000-L conditioner tank and a 1000-L Immobilised Biomass Reactor (IBR) (**Figure 1 (right)**). All the tanks were made in polypropylene.

The IBR is a flat-bottomed vessel filled with 700 L of polypropylene Pall<sup>®</sup> Ring supports (nominal diameter 15 mm, density 80 kg m<sup>-3</sup>, specific area 350 m<sup>2</sup> m<sup>-3</sup>, void fraction 0.9 m<sup>3</sup> m<sup>-3</sup>), colonized by activated sludge from the wastewater treatment plant installed at the pharmaceutical company itself. This bioreactor is also equipped with two air diffusers supplied with compressed air through independent pipes regulated with ball valves. Each diffuser can supply up to 10 N m<sup>3</sup> h<sup>-1</sup> of air. On-line pH and dissolved oxygen sensors are also placed in the conditioner tank return pipe. Both are connected to an automatic controller for automatic conditioner tank pH adjustment between 6.8 and 7.5 and dissolved oxygen between 4-6 mg L<sup>-1</sup> in the IBR by acting on two

pneumatic valves that feed air diffusers. The pH probe also has a Pt-100 sensor for monitoring the water outlet temperature (**Figure 2**).

This biological system was operated directly in continuous mode, because the purpose was to maintain the immobilised activated-sludge reactor working under the real conditions prevailing in a conventional wastewater treatment plant. It was operated in batch mode only during the start-up phase (IBR inoculation, bacteria fixation and growing, etc) (see Section 3.2). The industrial saline wastewater partially oxidized by photo-Fenton was discharged into the neutralisation tank (in **Figure 2**, valve (1) closed and (2) opened), which is a conical-bottomed vessel where water was roughly neutralised with concentrated NaOH and iron was settled and removed when necessary. Then the photo-pre-treated effluent was transferred to the conditioner tank, where the pH was automatically adjusted between 6.8 and 7.5 with 5% w/v NaOH throughout the biotreatment by a peristaltic pump. Then the effluent was pumped to the IBR, entering through a T-joint at the bottom, and water was sprayed up through the packed rings. The recirculation flow rate between the conditioner tank and the IBR was set at  $1.2 \text{ m}^3 \text{ h}^{-1}$  and the neutralised pre-treated effluent was continuously pumped from the neutralisation tank to the conditioner tank by a centrifugal pump ( $0.6\text{-}2 \text{ m}^3 \text{ day}^{-1}$ ). Once stationary state was reached between the conditioner tank and the IBR, the completely treated effluent (DOC between  $40\text{-}60 \text{ mg L}^{-1}$ , characteristic biological system end values for such industrial wastewater) was continuously discharged from the IBR.

During continuous biological operation, in which dissolved oxygen was kept between  $4\text{-}6 \text{ mg L}^{-1}$ , it was possible to calculate the volumetric gas (air)-liquid oxygen transfer coefficient ( $K_{La}$ ), a characteristic parameter commonly used in the description of aerobic biological reactors, using automatic data acquisition. During this stage,

dissolved oxygen clearly showed two-step consumption-absorption cycles, which made it possible to find  $K_L a$  from the liquid-phase oxygen mass balance (**Equation (2)**).

$$\left( \frac{dC_L}{dt} \right) = K_L a (C_s - C_L) - x \cdot q_{O_2}, \quad (2)$$

Where  $dC_L/dt$  is the oxygen accumulated in the liquid phase,  $K_L a (C_s - C_L)$  is the gas-to-liquid oxygen transfer rate,  $C_s$  is the concentration of oxygen in saturated conditions ( $8 \text{ mg L}^{-1}$ ),  $C_L$  is the concentration of oxygen in the liquid phase at time  $t$ ,  $x$  is the biomass concentration and  $q_{O_2}$  is the specific oxygen consumption.

## FIGURE 2

### 3. RESULTS AND DISCUSSION.

#### 3.1. Solar photo-Fenton treatment.

Prior to the combined photo-Fenton/biological treatment of MPG dissolved in an industrial wastewater, several studies had been performed to compare the pilot plant results (kinetics, hydrogen peroxide consumption, illumination time), with those from the pre-industrial-scale plant. The non-biodegradable compound<sup>28</sup>, MPG, was always dissolved in wastewater received from the pharmaceutical company where the demonstration plant was erected. This company uses sea water as process water so the wastewater is highly saline (for composition see Section 2.1). It is important to note that the MPG concentration of around  $600 \text{ mg L}^{-1}$  corresponded to a DOC of  $393 \text{ mg L}^{-1}$ , but DOC for the total mixture (MPG + wastewater) was around  $400\text{-}600 \text{ mg L}^{-1}$ . The DOC of the industrial wastewater changed continuously depending on the ongoing factory process, but it was always approximately between  $20$  and  $200 \text{ mg L}^{-1}$ .

**Figure 3 (a)** shows the degradation and mineralization of MPG dissolved in the industrial wastewater. The complete disappearance of MPG was attained after  $t_{30w} =$

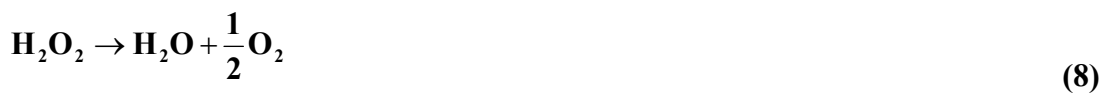
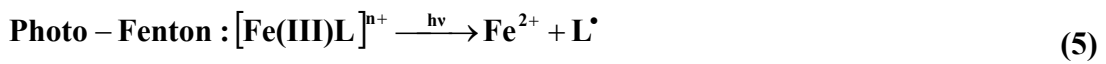
54 minutes of photo-Fenton treatment ( $\text{Fe}^{2+} = 20 \text{ mg}\cdot\text{L}^{-1}$ ) and DOC mineralization continued until  $t_{30w} = 105 \text{ min}$ , at which moment the mixture was biodegradable, as demonstrated in previously published pilot-plant-scale studies<sup>26,27</sup>. Quick decay of MPG and DOC at the beginning of the test (from  $t_{30w} = 0$  to approximately  $t_{30w} = 10$  minutes) was also observed. This decay was attributed to the formation of large amounts of foam from the carbon dioxide bubbles produced by pH adjustment at the beginning of the test ( $\text{pH}_0 = 2.3\text{-}2.5$ ). This foam retained large quantities of MPG and as foam disappeared during the photo-Fenton treatment, MPG redissolved. This strong decay may also have been caused by the Fenton reaction, as during the first minutes of the process it was governed mainly by **Reaction 3**, when the elimination of MPG was very fast. However, it was not possible to differentiate clearly between the disappearance of MPG retained by the foam or degraded by the Fenton reaction. In any case, it could be surmised that if  $76 \text{ mg L}^{-1}$  of DOC have been eliminated (from  $410 \text{ mg L}^{-1}$  to  $334 \text{ mg L}^{-1}$ ), the corresponding MPG concentration should be  $116 \text{ mg L}^{-1}$ , but  $267 \text{ mg L}^{-1}$  of MPG actually disappeared from the water (**Figure 3 (a)**). It should be remarked that during the first minutes of the process, mineralization should be very slow, as at the beginning of AOPs, organics are oxidised to other degradation products, but not mineralised. Therefore, the  $76 \text{ mg L}^{-1}$  of the above-mentioned DOC eliminated corresponding to  $116 \text{ mg L}^{-1}$  of MPG must all be retained in the foam. Therefore,  $464 \text{ g}$  of MPG were retained in the foam. This means that  $151 \text{ mg L}^{-1}$  were really decomposed (but not mineralised) during the first minutes of the treatment, mainly by **Reaction 4**. Once the  $\text{Fe}^{2+}$  was oxidised to  $\text{Fe}^{3+}$  the process was governed mainly by the slower **Reaction 5** and  $\text{Fe}^{3+}$  reduction thermal reactions (**Reaction 6**) (see also comments in Section 2.3.1).

### FIGURE 3

The kinetics of MPG degradation has also been studied assuming that the reaction between the  $\bullet\text{OH}$  radicals and the pollutant is the rate-determining step. MPG degradation may be described as a first-order reaction (**Equation 3**):

$$r = k_{OH} [\bullet\text{OH}]C = k_{ap}C \quad (3)$$

Where  $C$  is the MPG concentration,  $k_{OH}$  is the reaction rate constant,  $k_{ap}$  is a pseudo first-order constant, and  $[\bullet\text{OH}]$  is considered constant. This was confirmed by the linear behaviour of  $\ln(C_0/C)$  as a function of  $t_{30w}$ . The kinetic parameters found for MPG degradation are  $k_{ap} = 0.07 \text{ min}^{-1}$  and the initial reaction rate is  $r_0 = 44.4 \text{ mg L}^{-1} \text{ min}^{-1}$  ( $R^2 = 0.98$ ). This is much lower than in the pilot-plant tests with MPG dissolved in pure sea water ( $k_{ap} = 0.16 \text{ min}^{-1}$  and  $r_0 = 84.0 \text{ mg L}^{-1} \text{ min}^{-1}$ )<sup>26</sup>. This is because, on one hand, the MPG was dissolved in an industrial wastewater containing other unknown organics (20-200 mg DOC L<sup>-1</sup>) which were rivals of MPG for  $\bullet\text{OH}$  radicals and therefore, degradation of MPG was slower than when dissolved in pure sea water. On the other hand, the formation of large amounts of foam caused the same effect of retarding pollutant elimination by retaining MPG, which then leached out slowly (as explained above). Therefore, in industrial wastewater, the formation of foam could be highly detrimental to any AOP and should always be taken into account.



In all the pre-industrial-scale experiments performed, the required amount of hydrogen peroxide was added at the beginning of the process, as it has been demonstrated in pilot-plant tests to be the technically simplest dosing option for this industrial wastewater. Three different ways of dosing  $\text{H}_2\text{O}_2$  for the treatment of wastewater containing MPG had been studied at pilot-plant scale<sup>26</sup>: (i) the whole amount added at the beginning of the experiment, (ii) maintaining the  $\text{H}_2\text{O}_2$  concentration at  $50 \text{ mg L}^{-1}$  and, (iii) at  $400 \text{ mg L}^{-1}$ . An automatic PI feedback-control  $\text{H}_2\text{O}_2$  dosing system was used to keep the  $\text{H}_2\text{O}_2$  at a predefined concentration. The results showed a similar reaction rate with all three options. This was probably due to the fact, that in this particular case, the intermediate degradation products were strongly coloured (see **Figure 1** (left)), which provoked some inner filter effect towards the dissolved iron, that is, because of the absorption of the wastewater, the photochemical reactions involving dissolved iron were inhibited. Hence, the photochemical reduction of  $\text{Fe}^{3+}$  to  $\text{Fe}^{2+}$  was hindered in the catalytic iron cycle (**Reaction 5**) and parallel thermal reduction reactions of  $\text{Fe}^{3+}$  gained in importance (formation of  $[\text{Fe(III)(HO}_2)]^{n+}$  complex). These thermal reactions became the main reaction pathway for the rate-limiting reduction of  $\text{Fe}^{3+}$ , so a low hydrogen peroxide concentration negatively affected the overall degradation rate. When wastewater lost colour, the photo-reduction of  $\text{Fe}^{3+}$  complexes again became the rate-limiting step, as clearly seen in **Figure 3 (b)**.

Based on the results explained above, the technically simplest solution was used for all the demonstration plant experiments. Otherwise, the concentration of  $\text{H}_2\text{O}_2$  was always measured at the end of each photo-Fenton test in order to ensure its complete consumption during the process.

The consumption of hydrogen peroxide during photo-oxidation is also shown in **Figure 3 (a)**. The mass balance of the MPG degradation reaction is based on **Reactions 7-9**, where the combination of the mineralisation reaction (**Reaction 7**) and the decomposition of hydrogen peroxide (**Reaction 8**) are shown. According to **Reaction 9**, 72 mM of hydrogen peroxide should be consumed to mineralise 600 mg L<sup>-1</sup> of MPG, while 27 mM of hydrogen peroxide must be consumed for complete disappearance of the parent compound (**Figure 3 (a)**). When MPG was decomposed, a large amount of the organic content of MPG still remained in the water in the form of more oxidised organic compounds.

It is worth mentioning that the demonstration-scale H<sub>2</sub>O<sub>2</sub> consumption (27 mM) necessary for complete MPG degradation was similar to pilot-plant scale<sup>26</sup> (30-35 mM, 520 mg L<sup>-1</sup> of MPG), although the ratio of g H<sub>2</sub>O<sub>2</sub> consumed to g MPG degraded is one and a half times lower in the demonstration plant (1.5 g H<sub>2</sub>O<sub>2</sub> g MPG<sup>-1</sup>) than in the pilot plant experiments (2.5 g H<sub>2</sub>O<sub>2</sub> g MPG<sup>-1</sup>).

From **Reaction 8** it may be demonstrated that the nitrogen present in the MPG molecule was released mainly as ammonium (approximately 4 mM), which increased the solution pH from 2.3-2.5 at the beginning to 2.9 at the end of the treatment. The initial pH was therefore lower (2.3-2.5) than optimal for Photo-Fenton tests (2.8-2.9), avoiding Fe<sup>3+</sup> precipitation at pH higher than 3.

Temperature in the demonstration plant rises from dawn to become almost constant around afternoon, and decreases again during the evening ( $t_{30W} = 0$  was around 10:30 and  $t_{30W} = 105$  min was around 17:00). In **Figure 3 (b)**, it may be observed how water temperature varied from 21 to 37°C, at the same time global UV irradiation increased from 16 W m<sup>-2</sup> to 30 W m<sup>-2</sup> (partly cloudy from 12:00 to 13:30). Under these conditions, the photo-Fenton reaction rate varied during the treatment. Other authors

have described<sup>29</sup> differences of up to five times between 20 and 40°C. In recent work with model waste water by our group<sup>30</sup>, we found a similar effect (2.5 times faster at 35°C than at 20°C). It should also be mentioned that as temperature control is not economically feasible in a large-size solar photocatalytic plant, the effect of temperature and not just variation in solar UV power on the photo-Fenton reaction rate should be taken into account. This could lead to difficulties in the design of an adequate control system (for example, in determining the treatment time necessary before discharging to the biotreatment as a function of UV power and temperature) for solar photo-Fenton photocatalytic plants.

### **3.2. Immobilised Activated-Sludge biotreatment.**

Before beginning treatment of industrial wastewater containing MPG with the combined solar photo-Fenton / aerobic biological plant, the IBR must be equipped for biomass degradation of the photo-Fenton by-products. Optimal biological system conditions for continuous treatment of pre-oxidised effluents were implemented in batch mode.

Based on previous studies<sup>31,32</sup>, the IBR was inoculated with 1.5 m<sup>3</sup> of concentrated activated sludge from the aerobic tank of the pharmaceutical company's wastewater treatment plant and suspended in wastewater with a DOC of around 160 mg L<sup>-1</sup> and an ammonia concentration of 98 mg L<sup>-1</sup>. Recirculation was then maintained between the conditioner tank and the IBR for several days in order to ensure optimum fixation of the sludge on the polypropylene Pall<sup>®</sup> Ring supports (batch mode operation). The total suspended solids (TSS), DOC, ammonium and nitrate concentrations were measured daily. The TSS analysis assessed bacteria fixation on the supports during IBR inoculation. In approximately eight days TSS = 0, so proper bacteria fixation was

assured. At that moment, the normal influent from the factory wastewater treatment plant was added to the IBR in order to nourish and increase the biomass concentration fixed on the supports, and to favour the growth of a bacteria population specific to the pharmaceutical company's wastewater treatment plant. Two 1.5 m<sup>3</sup> doses of 130 mg DOC L<sup>-1</sup> (31 mg L<sup>-1</sup> of total nitrogen) and 260 mg DOC L<sup>-1</sup> (62 mg L<sup>-1</sup> of total nitrogen) respectively, were added. In both cases DOC was degraded down to a constant 60-65 mg L<sup>-1</sup> (in approximately two days), which is typical of background noise from physiological bacteria activity in industrial wastewater biological treatment. Furthermore, the nitrification process was working properly as practically no ammonium was detected (0.3 mg L<sup>-1</sup>) at constant low DOC. Therefore, correct bacteria fixation and biomass activity were proven.

Before starting continuous mode operation in the biological reactor, 0.5 m<sup>3</sup> of the system volume was replaced by the photo-Fenton pre-treated effluent twice (DOC = 210 mg L<sup>-1</sup>) in order to accustom bacteria to it, and avoid shock reducing future biomass activity. According to previous lab and pilot-plant-scale biological tests performed<sup>26,27</sup>, biodegradability enhancement of industrial wastewater containing MPG by photo-Fenton (Fe<sup>2+</sup> = 20 mg L<sup>-1</sup>) was accomplished when MPG was completely eliminated and DOC was reduced to approximately 50% of the initial value (see **Figure 3 (a)**). Therefore, the photo-Fenton treatment was continued in the demonstration plant to the same level (i.e., MPG completely degraded, 50% of initial DOC,  $t_{30W} = 105$  min), at which point, the pre-oxidised effluent was transferred to the neutralisation tank (see **Figure 2**) where the pH was manually adjusted to 7. Then, the biological system was drained and refilled twice with the effluent, where the DOC fell to the desired value (around 60 mg L<sup>-1</sup>, and TSS = 0) after around 4 or 5 days of biotreatment in batch mode. No mineral medium was added to the photo-Fenton pre-treated effluent as the sea

water matrix and the amount of ammonium generated from the degradation of MPG (approximately 4 mM), fulfilled the required C and N, P (8-10 mg/L depending on wastewater composition), Fe (from photo-Fenton) and Ca ratios for conventional biological systems as published elsewhere<sup>33</sup>: C:N:P of 100:20:5 and C:Fe:Ca of 100:2:2. Moreover, the demonstration biological plant was intended to simulate a real wastewater treatment plant based on supported biomass, so therefore, no additional mineral solution was used so conditions would be as realistic as possible. That is also the reason why inoculation and maintenance of activated sludge in the IBR was carried out under the same conditions as in the pharmaceutical company's wastewater treatment plant.

### **3.3. Combined solar photo-Fenton-aerobic biological system.**

Once demonstrated that the Immobilised Activated Sludge was able to eliminate the remaining DOC from the photo-Fenton pre-treated wastewater containing MPG, semi-continuous operation of the combined system began. Solar photo-Fenton treatment was always performed in batch mode, while the biological reactor was operated continuously. This mean that several photo-Fenton batches were carried on under the same conditions shown in **Figure 3** and fed to the neutralisation tank, from which the effluent was continuously pumped to the conditioner tank and through the IBR. As explained in Section 2.3.2., in stationary-state conditions, the completely treated effluent (at DOC around 60 mg L<sup>-1</sup>, TSS = 0) was continuously discharged from the IBR at the same flow rate as the inlet from the neutralisation tank.

**Figure 4** shows the specific volumetric organic load to the IBR, the DOC removed in the biological treatment and the variations in continuous flow (from 0.6 to 2 m<sup>3</sup> day<sup>-1</sup>). The DOC load and the DOC removed are calculated taking into account the continuous

inlet flow ( $\text{L day}^{-1}$ ), inlet DOC ( $\text{g m}^{-3}$ ), outlet DOC ( $\text{g m}^{-3}$ ) and the volume occupied by Pall ring® supports in the IBR ( $0.7 \text{ m}^3$ ), which is a volume representative of the amount of active biomass in the reactor.

#### **FIGURE 4**

The biological system started to operate in continuous mode on Day 21, and until Day 81 ( $600\text{-}800 \text{ L day}^{-1}$  from Day 21 to 64), the specific volumetric organic load of the IBR always remained around  $200 \text{ g m}^{-3} \text{ day}^{-1}$ . From Day 64 to 95, it was attempted to keep the continuous flow from the neutralisation tank to the conditioner tank between  $800$  and  $1000 \text{ L day}^{-1}$ . After Day 81 the initial MPG concentration dissolved in the industrial wastewater was raised to  $1 \text{ g L}^{-1}$  previous to the photo-oxidation step to achieve significantly higher organic loads in the IBR (from  $360$  to approximately  $1000 \text{ g m}^{-3} \text{ day}^{-1}$ ) without having to increase the number of batch treatments in the solar photo-Fenton stage proportionally. These photo-Fenton batches required more hydrogen peroxide ( $35 \text{ L}$ , corresponding to a  $77 \text{ mM}$  concentration) at the beginning of the process and a longer illumination time ( $t_{30w} = 180 \text{ min}$ ), to enhance the biodegradability of the pre-treated effluent (removal of  $50\%$  of initial DOC).

Finally, from day 95 to 100, the continuous flow was doubled to  $2000 \text{ L day}^{-1}$  in only five days. This last 20-day stage from Day 80 to 100 made it possible to determine the biological system's maximum treatment capacity. As observed from **Figure 4**, the amount of DOC removed in the biological system could generally said to be around  $2/3$  of the incoming DOC.

**Figure 5** shows DOC and nitrogen concentrations (from  $\text{NH}_4^+$ ) in the IBR outlet during continuous operation of the biological system. It is important to observe how outlet DOC remained between  $55$  and  $70 \text{ mg L}^{-1}$  until day 90 (within the limits for background noise from industrial wastewater bacteria activity), but from this point to the end, DOC

in the outlet increased to 110-120 mg L<sup>-1</sup>. At that moment, the specific volumetric organic load was more than doubled (470 g m<sup>-3</sup> day<sup>-1</sup>). There are two possible reasons for this increase in DOC, either the heterotrophic bacteria had reached the limit of their capacity and therefore, outlet DOC rose, or the more concentrated inlet contained more non-biodegradable substances. In order to find out which of these two assumptions was true, after Day 102 a batch was run with no further additions. During approximately 12 days of batch recirculation between the conditioner tank and the IBR, the DOC in the system gradually fell to around 84 mg L<sup>-1</sup>. This indicates that less degradation by the photo-Fenton treatment to increase the organic load fed to the IBR caused more hardly biodegradable compounds to be formed. It is worth remarking that DOC outlet concentration depends not only on the biodegradability of the effluent, but also on the dimensioning of the biological plant and the mean residence time inside the biological reactor. The mean residence time in the immobilised activated sludge bio-reactor studied in this work was approximately 17 hours when operating at 1 m<sup>3</sup> day<sup>-1</sup> (day 27 – 95) and 8 hours at 2 m<sup>3</sup> day<sup>-1</sup> (day 95 – 102). In this sense, the increase in the DOC outlet demonstrated the need to scale up slightly the bio-treatment to make the residence time in the biological reactor longer and allow fixed biomass to also degrade hardly biodegradable by-products from photo-Fenton treatment. It is therefore indispensable to thoroughly optimise these points for each real-size plant design based on the specific wastewater to be treated.

In the particular case of the demonstration plant and the real wastewater specifically tested in this work, maximum specific volumetric DOC degradation was found to be approximately 500 g m<sup>-3</sup>·day<sup>-1</sup> (**Figure 4**), which was more than three times higher than at pilot plant scale, mainly due to the strong increase in the amount of active biomass in the demonstration plant.

## FIGURE 5

Another important point in the aerobic biological treatment is that ammonia concentration in the effluent dropped, especially when the wastewater contained large amounts of  $\text{NH}_4^+$ . MPG contains 8.5% nitrogen and its degradation intermediates in pre-treated water would contain part of it. As mentioned in Section 3.1, nitrogen from the MPG molecule was released mainly as  $\text{NH}_4^+$ , and the wastewater in which MPG was dissolved also contained  $\text{NH}_4^+$ . The nitrogen from ammonium in the IBR outlet is also plotted in **Figure 5** where it can be observed that, from the first day to Day 71, the nitrogen concentration was between 30-40  $\text{mg L}^{-1}$  occasionally rising to 70  $\text{mg L}^{-1}$ . During this phase of continuous operation, automatically controlled dissolved oxygen in the IBR was kept between 4-6  $\text{mg L}^{-1}$  (see control description in Section 2.3.2), according to the pilot-plant experiments<sup>26</sup>. However, contrary to the pilot-plant results, in the demonstration plant, dissolved oxygen control was problematic, mainly because the air diffusers (at the bottom of the IBR) occasionally got plugged up when aeration stopped because the upper limit of oxygen concentration was reached. Consequently, air pressure had to be raised to unplug the air diffusers, causing violent bubbling through the immobilised biomass zone, and fixed biomass came unattached. Furthermore, the most common reasons for the increase in residual  $\text{NH}_4^+$  concentration are inhibiting substances, insufficient aeration and temperature too high. Temperatures in the IBR were never above 29°C, so it was not this parameter that was causing the problem. Therefore, automatic control of the dissolved oxygen was discontinued and was kept saturated (8  $\text{mg L}^{-1}$ ) in the IBR from Day 71 to the end of continuous operation. This situation was not economically optimised. Only when the specific volumetric organic load increased did the concentration of nitrogen rise, but after four days of biomass adaptation, ammonia concentration fell again.

As mentioned at the end of Section 2.3.2., during continuous biological operation it was possible to calculate the volumetric oxygen transfer coefficient ( $K_{La}$ ), because to the automatic control of dissolved oxygen kept it at 4-6 mg L<sup>-1</sup>.

Since aeration is stopped in the consumption phase and the oxygen transfer rate becomes null ( $K_{La}(C_s - C_L) = 0$ ), solution of **Equation 8** using the least squared error to fit the data gave a  $K_{La}$  of 20±5 h<sup>-1</sup>. This result is similar to those found for fluidized bed bioreactors with 1 vvm (volume per minute) and in stirred tank bioreactors at 400 rpm<sup>34</sup>. Such bioreactors are widely employed in biological systems for different purposes. Furthermore, continuous dissolved oxygen measurements showed that it always remained between 2 and 8 mg L<sup>-1</sup> when the automatic control was switched to continuous air supply. In fact, when the organic load was increased, the concentration of dissolved oxygen was always in that range. Otherwise, due to the polypropylene support packing inside the IBR, dissolved oxygen transfer in the column was not homogenous, and air bubbles would have to have preferred ways.

Finally, when the continuous flow was increased to 2 m<sup>3</sup> day<sup>-1</sup>, around 40 mg L<sup>-1</sup> of NO<sub>2</sub><sup>-</sup> was detected, showing that the system was not working properly. Considering that not only must DOC be degraded by the bio-treatment, but ammonia concentration must also be decreased, the final specific volumetric DOC degradation in the IBR (500 g m<sup>-3</sup> day<sup>-1</sup>) is the maximum treatment capacity for this demonstration plant under specific pre-treatment effluent conditions.

**Figure 6** shows the percentage of overall DOC removed by each step of the combined solar photo-Fenton / aerobic biological process, equivalent to the percentage of the initial DOC (100%) degraded in each step. Overall efficiency was in the range of 85-95% elimination of initial DOC, of which 50-65% was removed in the solar photo-Fenton treatment and 20-45% in the immobilised activated-sludge bio-treatment.

## FIGURE 6

It should also be mentioned that overall degradation efficiency depends not only on oxidation degree but also on the DOC inlet concentration.

## 4. CONCLUSIONS.

Compared to previously published pilot-plant-scale results for treatment of this saline industrial wastewater<sup>26,27</sup>, demonstration solar photo-Fenton pre-treatment successfully enhanced the biodegradability of the effluent in a reasonable length of time ( $t_{30W} = 105$  min). In view of the difficulties for very precise demonstration-plant scale testing, it should be mentioned that pilot plant tests are indispensable for accurate large-scale design parameters and operating procedures. It is also important for the demonstration plant to be constructed using a photoreactor design as similar as possible to the pilot plant so that results can be extrapolated. This is even more important with solar irradiation, as the source of energy is not constant.

The aerobic biological treatment was then able to reduce the DOC from the pre-oxidised effluent to specific bacteria activity ( $60-65 \text{ mg L}^{-1}$ ) by means of saline activated sludge fixed on propylene Pall ring® supports. The maximum specific volumetric DOC degradation in the biological treatment of the wastewater studied in this work was found to be  $500 \text{ g m}^{-3} \text{ day}^{-1}$  when a continuous flow rate of  $2 \text{ m}^3 \text{ day}^{-1}$  was maintained.

This two-step field treatment was operated in semi-continuous mode (solar photo-Fenton treatment in batch mode and the biological process in continuous mode), and overall efficiency was in the range of 85-95%, of which 50-65% was removed in the solar photo-Fenton treatment and 20-45% in the immobilised activated-sludge bio-treatment. It may therefore be concluded that the following points must be taken into account in future actual-size plants optimized for a specific industrial wastewater:

- a. Foam formation must be considered highly detrimental to apply photo-Fenton process.
- b. Apart from variation in solar UV power, temperature also affects the photo-Fenton reaction rate and should be taken into account in designing solar photocatalytic plant control systems.
- c. In the biological treatment, increased outlet organic content demonstrates the need of scaling up the bio-treatment by lengthening the residence time in the biological reactor to allow the fixed biomass to degrade part of the recalcitrant biodegradable photo-Fenton by-products.

## **5. ACKNOWLEDGMENTS.**

The authors wish to thank the European Commission for its financial support under the CADOX Project (Contract no. EVK1-CT-2002-00122), and to the Spanish Ministry of Education and Science for its financial support under the “Fotobiox” Project (CTQ2006-14743-C03-01/PPQ). They also wish to thank Mrs. Deborah Fuldauer for correcting the English. Isabel Oller would like to thank the Spanish Ministry of Education and Science for her Ph.D research grant.

## **6. REFERENCES.**

- (1) Gogate, P.R., Pandit, A.B. A review of comparative technologies for wastewater treatment I: oxidation technologies at ambient conditions. *Adv. Environ. Res.* **2004**, 8, 501.
- (2) Gogate, P.R.; Pandit, A.B. A review of comparative technologies for wastewater treatment II: Hybrid methods. *Adv. Environ. Res.* **2004**, 8, 553.
- (3) Devipriyas, S.; Yesodharan, S. Photocatalytic degradation of pesticide contaminants in water. *Sol. Energy Mater. Sol. Cells.* **2005**, 86, 309.

- (4) Herrmann, J.M. Heterogeneous photocatalysis: state of the art and present applications. *Top. Catal.* **2005**, 14(1-4), 48.
- (5) Pera-Titus, M.; García-Molina, V.; Baños, M.A.; Giménez, J.; Esplugas, S. Degradation of chlorophenols by means of advanced oxidation processes: a general review. *Appl. Catal. B: Environ.* **2004**, 47, 219.
- (6) Andreozzi, R.; Caprio, V.; Insola, A.; Marotta, R. Advanced oxidation processes (AOP) for water purification and recovery. *Catal. Today.* **1999**, 53, 131.
- (7) Malato, S.; Blanco, J.; Vidal, A.; Richter, C. Photocatalysis with solar energy at a pilot-plant scale: an overview. *Appl. Catal. B: Environ.* **2002**, 37, 1.
- (8) Bahnemann, D. Photocatalytic Water Treatment: Solar Energy Applications. *Sol. Energy.* **2004**, 77, 445.
- (9) Goswami, D.Y.; Vijayaraghavan, S.; Lu, S.; Tamm, G. New and emerging developments in solar energy. *Sol. Energy.* **2003**, 76, 33.
- (10) Blanco, J.; Fernández, P.; Malato, S. Solar Photocatalytic Detoxification and Disinfection of Water: Recent overview. *J. Sol. Energy Eng.* **2007**, 129, 4.
- (11) Pignatello, J.J.; Oliveros, E.; MacKay, A. Advanced oxidation processes for organic contaminant destruction based on the Fenton reaction and related chemistry. *Crit. Rev. Env. Sci. Technol.* **2006**, 36, 1.
- (12) Pulgarín, C.; Invernizzi, M.; Parra, S.; Sarria, V.; Polania, R.; Péringier, P. Strategy for the coupling of photochemical and biological flow reactors useful in mineralization of biorecalcitrant industrial pollutants. *Catal. Today.* **1999**, 54, 341.
- (13) Kositzki, M.; Poullos, I.; Malato, S.; Cáceres, J; Campos, A. Solar photocatalytic treatment of synthetic municipal wastewater. *Water Res.* **2004**, 38, 1147.

- (14) Machado, A. E. H.; Xavier, T. P.; Rodrigues de Souza, D.; de Miranda, J. A.; Mendonça Duarte, E. T. F.; Ruggiero, R.; de Oliveira, L.; Sattler, C. Solar photo-Fenton treatment of chip board production waste water. *Sol. Energy*. **2004**, 77, 583.
- (15) Sattler, C.; Funken, K.-H.; de Oliveira, L.; Tzschirner, M.; Machado, A.E.H. Paper Mill Wastewater Detoxification by Solar Photocatalysis. *Wat. Sci. Technol.* **2004**, 49 (4), 189.
- (16) Farré, M. J.; Franch, M. I.; Malato, S.; Ayllón, J. A.; Peral, J.; Doménech, X. Degradation of some biorecalcitrant pesticides by Homogeneous and Heterogeneous Photocatalytic Ozonation. *Chemosphere*. **2005**, 58, 1127.
- (17) Oller, I.; Fernández-Ibáñez, P.; Maldonado, M.I; Pérez-Estrada, L.; Gernjak, W.; Pulgarín, C.; Passarinho, P.C.; Malato, S. Solar heterogeneous and homogeneous photocatalysis as a pre-treatment option for biotreatment. *Res. Chem. Interm.* **2007**, 33(3-5), 407.
- (18) Esplugas, S.; Ollis, D.F. Economic Aspects of Integrated (Chemical + Biological) Processes for Water Treatment. *J. Adv. Oxid. Technol.* **1997**, 2 (1), 197.
- (19) Marco, A.; Esplugas, S.; Saum, G. How and why combine chemical and biological processes for wastewater treatment. *Wat. Sci. Technol.* **1997**, 35, 321.
- (20) Mantzavinos, D.; Psillakis, E. Enhancement of biodegradability of industrial wastewaters by chemical oxidation pre-treatment. *J. Chem. Technol. Biotechnol.* **2004**, 79, 431.
- (21) Bressan, M; Liberatorre, L.; D'Alessandro, L.; Tonucci, L.; Belli, C.; Ranalli, G. Improved combined chemical and biological treatments of olive oil mill wastewaters. *J. Agric. Food Chem.* **2004**, 52, 1228.

- (22) Mantzavinos, D.; Kalogerakis, N. Treatment of olive mill effluents Part I. Organic matter degradation by chemical and biological processes-an overview. *Environ. Technol.* **2005**, 31, 289.
- (23) Heinzle, E.; Geiger, F.; Fahmy, M.; Kut, O.M. Integrated Ozonation-Biotreatment of Pulp Bleaching Effluents Containing Chlorinated Phenolic Compounds. *Biotechnol. Prog.* **1992**, 8, 67.
- (24) Sarria, V.; Deront, M.; Péringer, P.; Pulgarín, C. Degradation of a biorecalcitrant dye precursor present in industrial wastewaters by a new integrated iron (III) photoassisted-biological treatment. *Appl. Catal. B: Environ.* **2003**, 40 (3), 231.
- (25) Contreras, S.; Rodríguez, M.; AlMomani, F.; Sans, C.; Esplugas, S. Contribution of the ozonation pre-treatment to the biodegradation of aqueous solutions of 2,4-dichlorohenol. *Wat. Res.* **2003**, 37, 3164.
- (26) Oller, I.; Malato, S.; Sánchez-Pérez, J.A.; Gernjak, W.; Maldonado, M.I.; Pérez-Estrada, L.A.; Pulgarín, C. A Combined solar photocatalytic-biological field system for the mineralization of an industrial pollutant at pilot scale. *Catal. Today.* **2007**, 122, 150.
- (27) Malato, S.; Blanco, J.; Maldonado, M.I.; Oller, I.; Gernjak, W.; Pérez-Estrada, L. Coupling solar photo-Fenton and biotreatment at industrial scale: Main results of a demonstration plant. *J. Haz. Mat.* **2007**, in press.
- (28) M. Lapertot, C. Pulgarín. Biodegradability assessment of several priority hazardous substances: Choice, application and relevance regarding toxicity and bacterial activity. *Chemosphere* 65 (2006) 682-690
- (29) Sagawe, G.; Lehnard, A.; Lüber, M.; Bahnemann D. The insulated solar Fenton hybrid process: Fundamental investigations. *Helv. Chem. Acta.* **2001**, 84, 3742.

- (30) Gernjak, W.; Fuerhacker, M.; Fernández-Ibañez, P; Blanco, J.; Malato, S. Solar photo-Fenton treatment Process parameters and process control. *Appl. Catal. B: Environ.* **2006**, 64, 121.
- (31) Sarria, V.; Denfack, S.; Guillod, O.; Pulgarín, C. An innovative coupled solar-biological system at field pilot scale for the treatment of biorecalcitrant pollutants. *J. Photochem. Photobiol., A: Chemistry.* **2003**, 159, 89.
- (32) Farré, M.J.; Doménech, X.; Peral, J. Assessment of photo-Fenton and biological treatment coupling for Diuron and Linuron removal from water. *Water Res.* **2006**, 40, 2533.
- (33) Henze, Harremoës. Wastewater treatment. Biological and Chemical Processes. *La Cour Jansen and Arvin, 3<sup>rd</sup> Ed., Springer.* **2002**.
- (34) Casas López, J.L.; Rodríguez Porcel, E.M.; Oller Alberola, I.; Ballesteros Martín, MM.; Sánchez Pérez, J.A.; Fernández Sevilla, J.M.; Chisti, Y. Simultaneous Determination of Oxygen Consumption Rate and Volumetric Oxygen Transfer Coefficient in Pneumatically Agitated Bioreactors. *Ind. Eng. Chem. Res.* **2006**, 45, 1167.

**Figure captions:**

**Figure 1.** Views of the combined solar photo-Fenton /biological demonstration plant. Solar collector field (left), conditioner tank and Immobilised Biomass Reactor (right).

**Figure 2.** Simplified flow diagram of the demonstration combined photo-Fenton/aerobic biological plant.

**Figure 3. (a)** Degradation and mineralization of MPG dissolved in saline industrial wastewater by photo-Fenton with  $20 \text{ mg L}^{-1}$  of  $\text{Fe}^{2+}$ . Hydrogen peroxide consumption is also shown. **(b)** Temperature and global UV radiation during the experiment.

**Figure 4.** Specific volumetric organic load of IBR, continuous flow from the neutralisation tank to the conditioner tank and DOC removed per  $\text{m}^3$  occupied by polypropylene supports in the IBR.

**Figure 5.** DOC and nitrogen from  $\text{NH}_4^+$  in the IBR outlet during continuous operation.

**Figure 6.** Percentage of DOC removed by photo-Fenton and by biological treatment (IBR). The percentage of DOC remaining in the IBR outlet is also shown.

**Figure 1**



Figure 2

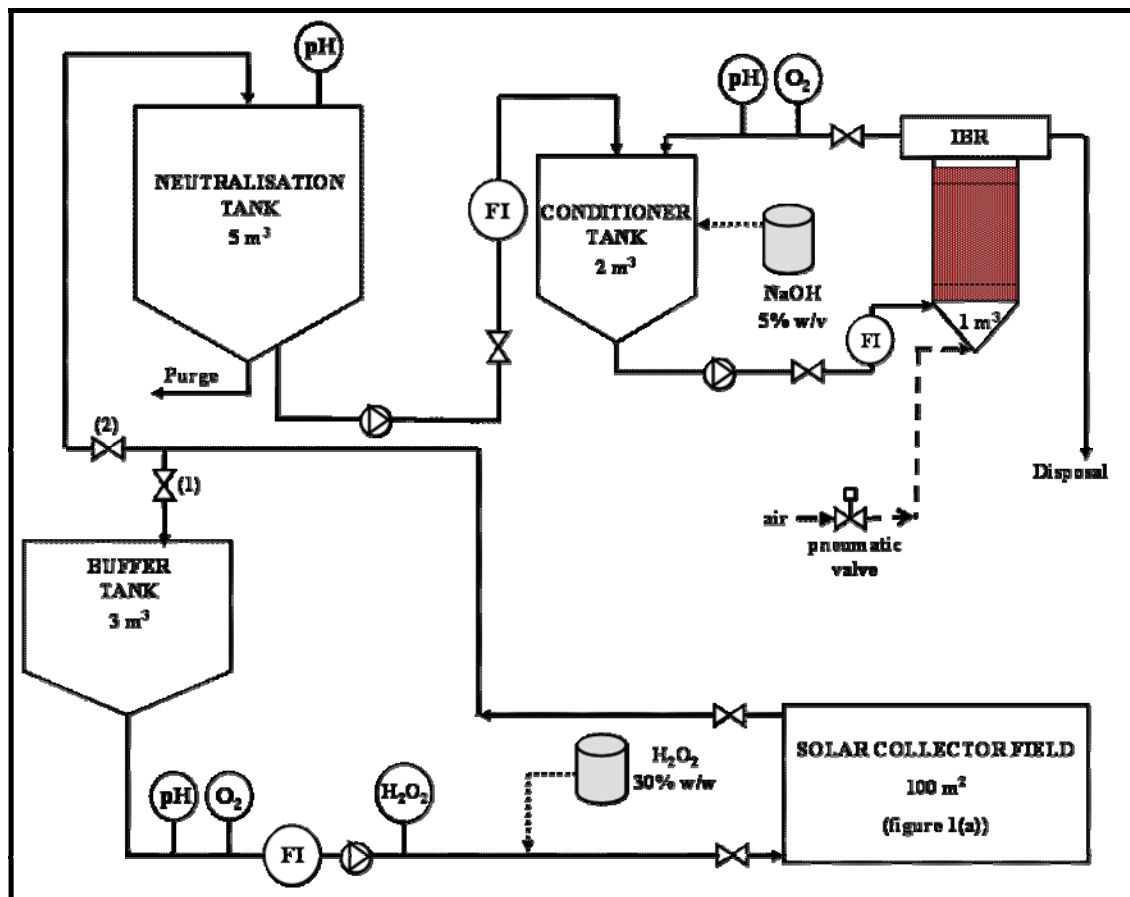


Figure 3

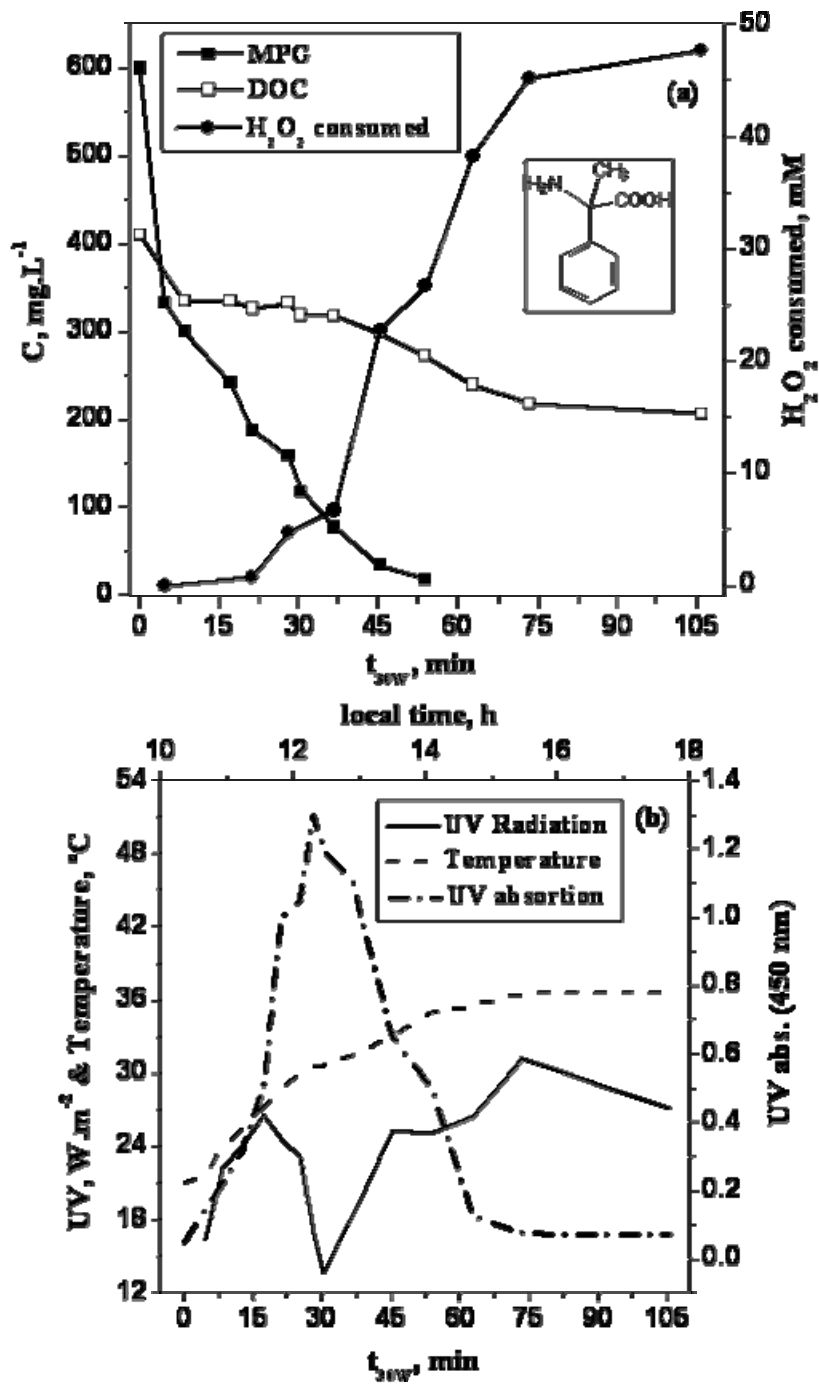


Figure 4

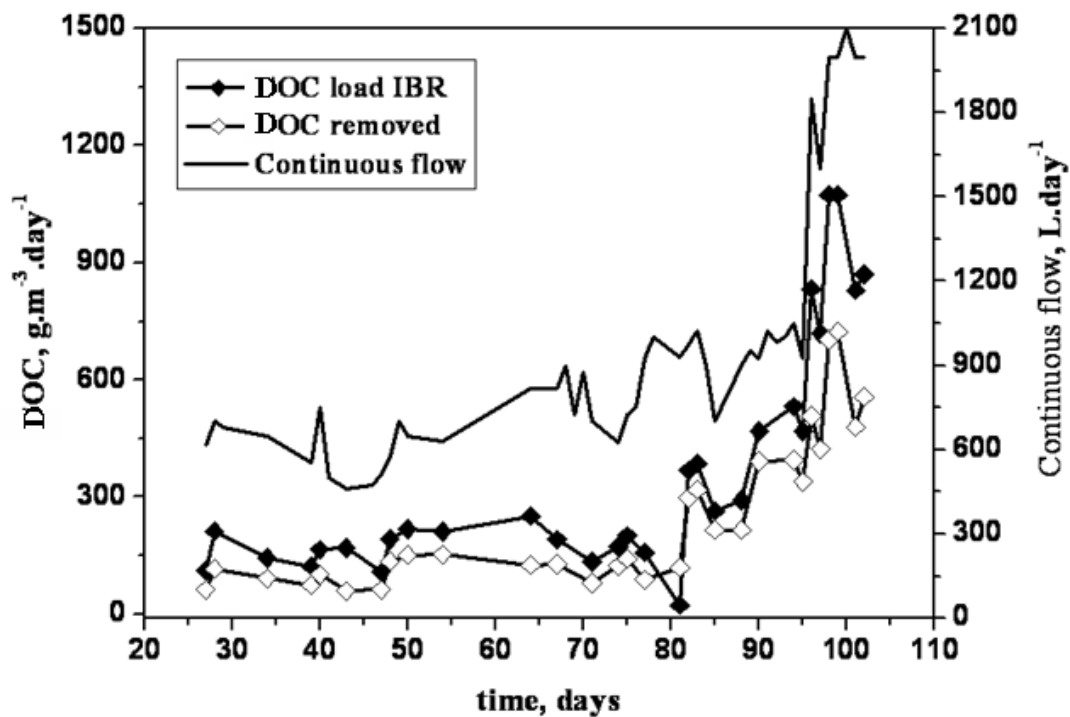


Figure 5

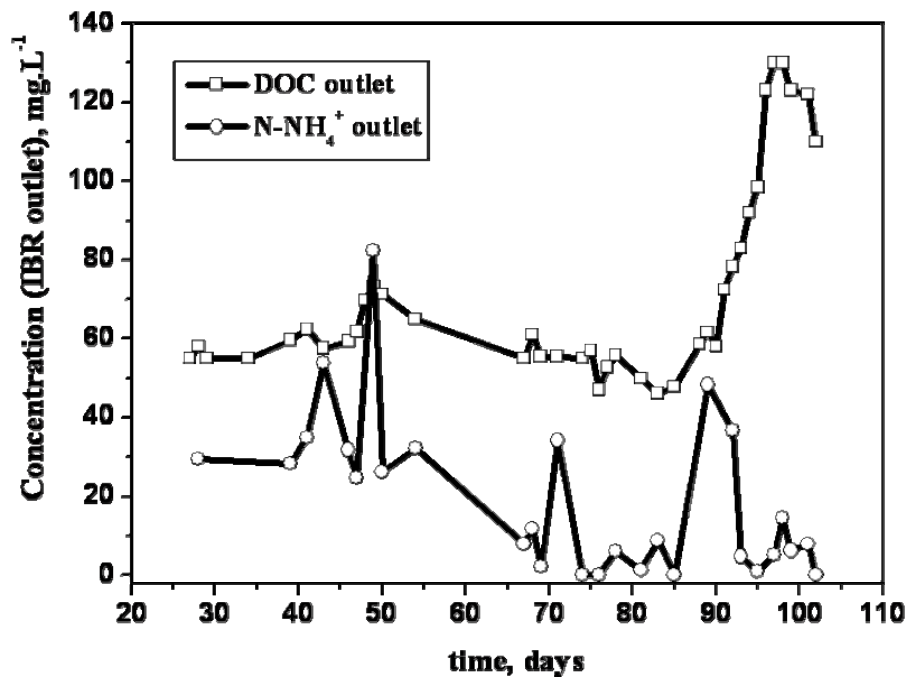


Figure 6

